

The Ferrocene–Lithium Cation Complex in the Gas Phase

Arantxa Irigoras, Jose M. Mercero, Iñaki Silanes, and Jesus M. Ugalde*

Contribution from the Kimika Fakultatea, Euskal Herriko Unibertsitatea, P. K. 1072, 20080 Donostia, Euskadi, Spain

Received August 21, 2000. Revised Manuscript Received January 29, 2001

Abstract: The stable isomers of the ferrocene–lithium cation gas-phase ion complex have been studied with the hybrid density functional theory. The method of calculation chosen has been tested checking its performance for the more studied protonated ferrocene species. Our calculations demonstrate that the procedure used is reliable. We have found two isomers of the ferrocene–lithium cation complex separated by a barrier of 25.6 kcal/mol. The most stable isomer of this complex has Li⁺ on-top of one of the cyclopentadienyls, while in the least stable isomer Li⁺ binds the central iron metal. The latter isomer has been characterized as a planetary system in the sense that Li⁺ has one thermally accessible planar orbit around the central ferrocene moiety. Our calculations lead to a value of ferrocene's gas-phase lithium cation basicity of 37.4 kcal/mol for the on-top complex and 29.4 kcal/mol for the metal-bound complex.

I. Introduction

Gas-phase Li⁺ was long ago known to be a ubiquitous cation that yields strong, mostly electrostatic interactions with neutral species.¹

Recently, it has regained interest due to its ability to form *planetary systems*. This term, coined by Abboud et al.² for P₄•••Li⁺, refers to complexes between Li⁺ and a neutral species where the cation has closed, thermally accessible paths resembling *orbits*, revolving around the central neutral species. Although *planetary systems* were described earlier in the literature,^{3–5} the complex synthesized and characterized by Abboud et al. has the peculiarity that the *orbiting* of Li⁺ around the central P₄ unit is 4-fold degenerate due to its high symmetry.

On the other hand, the reactivity of ferrocene toward electrophiles is also a very active field of research. In particular, the nucleophilic behavior of ferrocene has been studied in great detail by Mayor-López et al.⁶ following earlier experimental work by Rosenblum et al.⁷ and Cunningham,^{8–10} who found that hard electrophiles, like proton and acetylene, are most likely to bind to the central iron atom of the ferrocene (an *endo* attack), whereas soft electrophiles (mercury) prefer to bind to the cyclopentadienyl ring of the ferrocene moiety (an *exo* attack). In view of the interest shown by the experimentalists on the electrophilic behavior of metallocenes,¹¹ it should be of some interest to learn more on the interactions between Li⁺ and

ferrocene, since the latter is well-known to constitute an ideal prototype for metallocenes.

Finally, given the importance of the interactions of acids and bases in chemistry and in particular of the gas-phase proton and alkali metal transfer equilibria,¹² this work aims to contribute to the building of a reliable data set concerned with the intrinsic basicity of the lithium cation.¹³

II. Computational Methods

All structures reported in this paper were first optimized and then followed by a frequency calculation at the same level of theory to assess whether each corresponds to a real minimum (all force constants positive) or to a transition state (all but one positive force constant) and to estimate the zero-point vibrational energy correction (ZPVE). The whole set of completely optimized geometries and vibrational frequencies is available in the Supporting Information.

Calculations have been carried out with the GAUSSIAN98/DFT¹⁴ suite of programs. Also Natural Bonding Orbital (NBO)^{15,16} calculations have been done to give additional insight into the bonding properties of some of the structures.

(11) Chirik, P. J.; Bercaw, J. E. In *Metallocenes. Synthesis, Reactivity and Applications*; Toni, A., Halterman, R. L., Eds.; Wiley-VCH: Weinheim, Germany, 1998; pp 111–152.

(12) Hunter, E. P. L.; Lias, S. G. *J. Phys. Chem. Ref. Data* **1998**, *27*, 413–656.

(13) Burk, P.; Koppel, I. A.; Koppel, I.; Kurg, R.; Gal, J. F.; Maria, P. C.; Herreros, M.; Notario, R.; Abboud, J. L.; Anvia, F.; Taft, R. W. *J. Phys. Chem. A* **2000**, *104*, 2824.

(14) Frisch, M. J.; Trucks, G. W.; Schlegel, H. B.; Scuseria, G. E.; Robb, M. A.; Cheeseman, J. R.; Zakrzewski, V. G.; Montgomery, J. A., Jr.; Stratmann, R. E.; Burant, J. C.; Dapprich, S.; Millam, J. M.; Daniels, A. D.; Kudin, K. N.; Strain, M. C.; Farkas, O.; Tomasi, J.; Barone, V.; Cossi, M.; Cammi, R.; Mennucci, B.; Pomelli, C.; Adamo, C.; Clifford, S.; Ochterski, J.; Petersson, G. A.; Ayala, P. Y.; Cui, Q.; Morokuma, K.; Malick, D. K.; Rabuck, A. D.; Raghavachari, K.; Foresman, J. B.; Cioslowski, J.; Ortiz, J. V.; Stefanov, B. B.; Liu, G.; Liashenko, A.; Piskorz, P.; Komaromi, I.; Gomperts, R.; Martin, R. L.; Fox, D. J.; Keith, T.; Al-Laham, M. A.; Peng, C. Y.; Nanayakkara, A.; Gonzalez, C.; Challacombe, M.; Gill, P. M. W.; Johnson, B.; Chen, W.; Wong, M. W.; Andres, J. L.; Gonzalez, C.; Head-Gordon, M.; Replogle, E. S.; Pople, J. A. *Gaussian 98*, Revision A.5, 1998.

(15) Reed, A. E.; Curtiss, L.; Weinhold, F. *Chem. Rev.* **1988**, *88*, 899.

(16) Glendening, A. E.; Reed, A. E.; Carpenter, J. E.; Weinhold, F. *NBO*, Version 3.1.

(1) Sapse, A. M.; Schleyer, P. v. R. *Lithium Chemistry: A Theoretical and Experimental Overview*; John Wiley: New York, 1995.

(2) Abboud, J. L. M.; Alkorta, I.; Dávalos, J. Z.; Gal, J. F.; Herreros, M.; Maria, P. C.; Mó, O.; Molina, M. T.; Notario, R.; Yañez, M. *J. Am. Chem. Soc.* **2000**, *122*, 4451.

(3) Blomberg, M. R. A.; Siegbahn, P. E. R.; Svensson, M. *J. Phys. Chem.* **1994**, *98*, 2062.

(4) Midland, M. M.; Morton, T. H. *J. Am. Chem. Soc.* **1993**, *115*, 9596.

(5) Illies, A. J.; Morton, T. H. *Int. J. Mass Spectrom. Ion. Proc.* **1997**, *167/168*, 431.

(6) Mayor-López, M.; Weber, J.; Mannfors, B.; Cunningham, A. F., Jr. *Organometallics* **1998**, *17*, 4983.

(7) Rosenblum, M.; Santer, J. O.; Howells, W. G. *J. Am. Chem. Soc.* **1963**, *85*, 1450.

(8) Cunningham, A. F., Jr. *J. Am. Chem. Soc.* **1991**, *113*, 4864.

(9) Cunningham, A. F., Jr. *Organometallics* **1994**, *13*, 2480.

(10) Cunningham, A. F., Jr. *Organometallics* **1997**, *16*, 1114.

The experience of this group^{17–22} shows that Density Functional Theory (B3LYP functional)^{23–25} with the DZVP basis sets given by Salahub et al.^{26,27} as a starting point and reoptimization with the TZVP+G(3df,2p) quality basis set is a reasonable choice for optimization and frequency calculations of systems containing first-row transition metals. The triple- ζ quality basis set, TZVP+G(3df,2p), used for the metal was that given by Schäfer, Hubert, and Ahlrichs,²⁸ supplemented with a diffuse s function (with an exponent 0.33 times that of the most diffuse s function on the original set), two sets of p functions optimized by Wachters²⁹ for the excited states, one set of diffuse pure angular momentum d functions (optimized by Hay),³⁰ and three sets of uncontracted pure angular momentum f functions, including both tight and diffuse exponents, as recommended by Ragavachari and Trucks.³¹ For the carbon, hydrogen, and lithium atoms the 6-311++G(2df,2p) basis set of Pople et al.³² was used.

III. Preliminary Calculations

The choice of the B3LYP functional is largely motivated by its satisfactory performance^{33–40} for transition metal containing systems. Other methods such as CASPT2⁴¹ and CCSD(T)⁴² have also been considered. However, since they require very large basis sets to yield accurate results,³⁵ the computational requirements became prohibitive very rapidly, so they were discarded.

Nevertheless, we would like to assess further the reliability of our chosen B3LYP procedure by calculating a number of selected properties of both the ferrocene and the protonated ferrocene and comparing the obtained results with earlier theoretical and experimental data.

A. Ferrocene. Although most theoretical procedures predict results in agreement with the available experimental data, that the eclipsed configuration of ferrocene is slightly more stable than staggered, the prediction of the metal–ligand equilibrium

(17) Irigoras, A.; Ugalde, J. M.; Lopez, X.; Sarasola, C. *Can. J. Chem.* **1996**, *74*, 1824–1829.

(18) Irigoras, A.; Fowler, J. E.; Ugalde, J. M. *J. Phys. Chem. A* **1998**, *102*, 293.

(19) Irigoras, A.; Fowler, J. E.; Ugalde, J. M. *J. Am. Chem. Soc.* **1999**, *121*, 574.

(20) Irigoras, A.; Fowler, J. E.; Ugalde, J. M. *J. Am. Chem. Soc.* **1999**, *121*, 8549–8558.

(21) Irigoras, A.; Elizalde, O.; Silanes, I.; Fowler, J. E.; Ugalde, J. M. *J. Am. Chem. Soc.* **2000**, *122*, 114.

(22) Irigoras, A.; Fowler, J. E.; Ugalde, J. M. *J. Am. Chem. Soc.* **2000**, *122*, 1411.

(23) Becke, A. D. *Phys. Rev. A* **1988**, *38*, 3098.

(24) Becke, A. D. *J. Chem. Phys.* **1993**, *98*, 5648.

(25) Lee, C.; Yang, W.; Parr, R. G. *Phys. Rev. B* **1988**, *37*, 785.

(26) Sim, F.; Salahub, D. R.; Chim, S.; Dupuis, M. *J. Chem. Phys.* **1991**, *95*, 4317.

(27) Godbout, N.; Salahub, D. R.; Andzelm, J.; Wimmer, E. *Can. J. Chem.* **1992**, *70*, 560.

(28) Schäfer, A.; Hurbert, C.; Ahlrichs, R. *J. Chem. Phys.* **1994**, *100*, 5829.

(29) Wachters, A. J. *J. Chem. Phys.* **1970**, *52*, 1033.

(30) Hay, P. J. *J. Chem. Phys.* **1971**, *66*, 4377.

(31) Raghavachari, K.; Trucks, G. W. *J. Chem. Phys.* **1989**, *91*, 1062.

(32) Krishnan, J. S.; Binkley, J. S.; Seeger, D.; Pople, J. A. *J. Chem. Phys.* **1980**, *72*, 650.

(33) Ricca, A.; Bauschlicher, C. W. *J. Phys. Chem.* **1994**, *98*, 12899.

(34) Bauschlicher, C. W.; Maitre, P. *J. Phys. Chem.* **1995**, *99*, 3444.

(35) Siegbahn, P. E. M. *Adv. Chem. Phys.* **1996**, *43*, 333.

(36) Bauschlicher, C. W.; Ricca, A.; Partridge, H.; Langhoff, S. *Recent Advances in Density Functional Theory. Part II*; World Scientific Publishing Co.: Singapore, 1997.

(37) Sodupe, M.; Branchadell, V.; Rosi, M.; Bauschlicher, C. W. *J. Phys. Chem. A* **1997**, *101*, 7854–7859.

(38) Hartmann, M.; Clark, T.; van Eldik, R. *J. Am. Chem. Soc.* **1997**, *119*, 7843.

(39) Filatov, M.; Shaik, S. *J. Phys. Chem. A* **1998**, *102*, 3835.

(40) Pavlov, M.; Siegbahn, P. E. M.; Sandström, M. *J. Phys. Chem. A* **1998**, *102*, 219.

(41) Andersson, K.; Malmqvist, P. Å.; Roos, B. O.; Sadlej, A. J.; Wolinski, K. *J. Phys. Chem.* **1990**, *94*, 5483.

(42) Raghavachari, K.; Trucks, G. W.; Pople, J. A.; Head-Gordon, M. *Chem. Phys. Lett.* **1989**, *157*, 479.

Table 1. Iron–Cyclopentadienyl Vertical Distance, in Å, in the Ferrocene Molecule^a

method	distance
B3LYP/DZVP	1.672
B3LYP/TZVP+G(3df,2p)	1.689
experiment [51]	1.66
HF [43]	1.88
HF [52]	1.872
MP2/[16s12p8d6f](58) [52]	1.489
MP2-R12/[16s12p8d6f](58) [52]	1.481
MP2/[16s12p8d6f](66) [52]	1.474
MP2-R12/[16s12p8d6f](66) [52]	1.468
MCPF/[4s4p3d1f](66) [44]	1.684
MP2 ^b [44]	1.65–1.67
MCPF ^c [44]	1.727
MCPF ^d [44]	1.865
CASSCF(10,10)/[6s5p4d2f] [53]	1.716
CASPT2(10,10)/[6s5p4d2f] (58) [53]	1.617
CASPT2(10,10)/[6s5p4d2f] +BSSE (58) [53]	1.643
CCSD/DZP(66) [45]	1.675
CCSD/DZP(96) [45]	1.672
CCSD/TZV2P+f(66) [45]	1.672
CCSD/TZV2P+f(96) [45]	1.664
CCSD(T)/DZP (66) [45]	1.665
CCSD(T)/TZV2P+f(66) [45]	1.660

^a The number of correlated electrons is given in parentheses. Reference numbers are given in squared brackets. ^b Values calculated replacing the iron atom by a +2 point charge. ^c Single excitations excluded. ^d Single excitations included.

distance in ferrocene has been reported as notoriously difficult.^{43–45}

Park and Almöf⁴⁴ noted that the metal–ligand distance is a problem in ferrocene because of the dynamic correlation. Later Koch and co-workers⁴⁵ confirmed that claim and suggested that both a size-extensive treatment of correlation effects beyond MP2 and a basis set capable of reproducing the correct equilibrium structure within 0.01 Å are needed to yield accurate results of the molecular structure of ferrocene.

All the values of the metal-to-ring distance of ferrocene found in the literature are listed in Table 1, along with our completely optimized B3LYP/DZVP and B3LYP/TZVP+G(3df,2p) data. From inspection of Table 1, we conclude that our procedure yields metal–ligand distances that are in reasonable agreement with experiment and highly accurate ab initio molecular orbital methods.

The heterolytic dissociation energy of reaction 1 is another difficult property to estimate theoretically.⁴⁶



Recently, several studies have been carried out at various levels of theory to obtain a feasible prediction of this property. The most recent values from the literature along with our ones are collected in Table 2.

The calculations show that B3LYP with a large enough basis set compares favorably to other ab initio procedures such as CASPT2 and CCSD(T). Our best result of 656 kcal/mol for the dissociation energy leads to a value of 648 kcal/mol for the dissociation enthalpy at 298 K, which overestimates slightly the experimental value⁴⁷ of 635 ± 6 kcal/mol.

(43) Lüthi, H. P.; Ammeter, J.; Almlöf, J.; Korsell, K. *Chem. Phys. Lett.* **1980**, *69*, 540.

(44) Park, C.; Almlöf, J. *J. Chem. Phys.* **1991**, *95*, 1829–1833.

(45) Koch, H.; Jørgensen, P.; Helgaker, T. *J. Chem. Phys.* **1996**, *104*, 9528–9530.

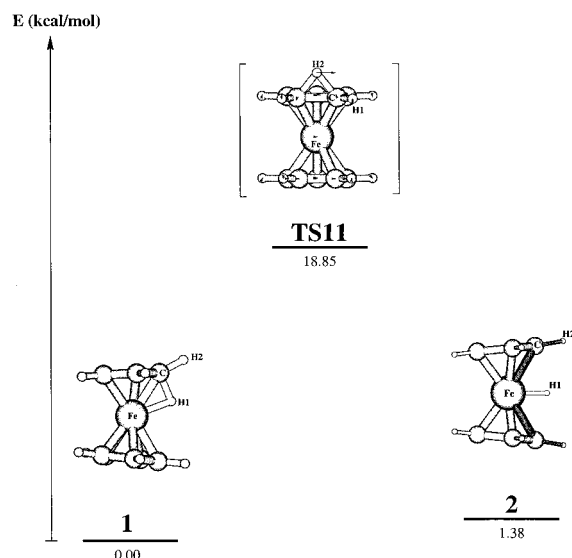
(46) Mayor-López, M. J.; Weber, J. *Chem. Phys. Lett.* **1997**, *281*, 226–232.

(47) Corliss, C.; Sugar, J. *J. Phys. Chem. Ref. Data* **1982**, *11*, 135.

Table 2. Zero-Point Vibrational Energy Corrections (Δ ZPVE), Basis Set Superposition Error Corrections (BSSE), and Dissociation Energies (D_0), in kcal/mol, for the Heterolytic Reaction 1^a

method	ZPVE	BSSE	D_0
B3LYP/DZVP	-8.008	10.350	676
B3LYP/TZVP+G(3df,2p)	-7.913	1.962	656
SCF [53]		9	570
SCF [45]		6	572
MP2(58) [53]		28	706
MP2(58) [45]		15	699
MP2(66) [53]		45	732
MP2(66) [45]		20	724
CCSD(66) [45]			706
CCSD(T)(66) [45]			728
CASSCF [53]			650
CASPT2 [53]			745
Theoretical Estimate(CASPT2) [52]	-7		657
Theoretical Estimate(CCSD(T)) [52]	-7		653
LDA [46]	-7	7	733
BPW91 [46]	-7	6	663

^a The number of correlated electrons is given in parentheses. Reference numbers are given in squared brackets.

**Figure 1.** The stationary points of $Cp_2Fe \cdots H^+$ at the B3LYP/TZVP+G(3df,p) level of theory. Energies given are in kcal/mol and are relative to structure **1**. For the transition state **TS11**, arrows show the atomic displacements corresponding to the negative force constant mode.

B. Protonated Ferrocene. Protonated ferrocene has been studied experimentally by Curphey et al.⁴⁸ and Meot-Ner,⁴⁹ and theoretically by Mayor-López et al.^{6,50}

We have been able to characterize two stable structures, almost degenerate in energy on the potential energy surface of the protonated ferrocene. Our most stable structure (**1** in Figure 1) is best characterized as a two electron-three center hydrogen bonded species. Structure **2** of Figure 1 corresponds to the metal-protonated ferrocene and is only 1.38 kcal/mol higher in energy at our best level of theory. These results agree with the recent very accurate CCSD(T) calculations of Mayor-López et al.⁵⁰ and lend further support to our method. Additionally, we have

(48) Curphey, T. J.; Santer, J. O.; Rosenblum, M.; Richards, J. H. *J. Am. Chem. Soc.* **1960**, *82*, 5249.

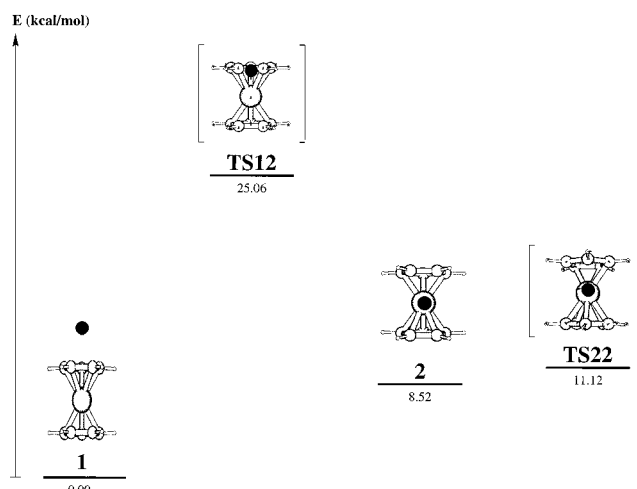
(49) Meot-Ner, M. *J. Am. Chem. Soc.* **1989**, *111*, 2830.

(50) Mayor-López, M.; Lüthi, H. P.; Koch, H.; Morgatini, P. Y.; Weber, J. *J. Chem. Phys.* **2000**, *113*, 8009.

(51) Haaland, A. W. *Top. Curr. Chem.* **1975**, *53*, 1.

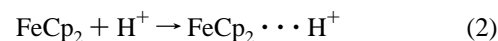
(52) Klopper, W.; Lüthi, H. P. *Chem. Phys. Lett.* **1996**, *262*, 546–552.

(53) Pierloot, K.; Persson, B. J.; Roos, B. O. *J. Phys. Chem.* **1995**, *99*, 3465–3472.

**Figure 2.** The stationary points of $Cp_2Fe \cdots Li^+$ at the B3LYP/TZVP+G(3df,p) level of theory. Energies given are in kcal/mol and are relative to structure **1**. For the transition states **TS12** and **TS22**, arrows indicate the atomic displacements corresponding to the negative force constant mode. Lithium is shown in black.

also been able to find the transition state associated with the migration of the proton from one carbon to an adjacent one on the same cyclopentadienyl. This structure is shown as **TS11** in Figure 1. It lies 18.8 kcal/mol above the stable minimum **1**.

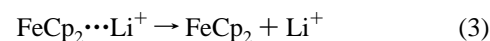
Finally we have also calculated the B3LYP proton affinity of ferrocene with our two basis sets, namely DZVP and TZVP++G(3df,2p). The proton affinity is defined as the negative of the change of enthalpy at room temperature for the reaction



For the most stable isomer of protonated ferrocene, both calculations yield extremely good values for the proton affinity, 207.6 kcal/mol and 207.2 kcal/mol at the B3LYP/DZVP and B3LYP/TZVP++G(3df,2p) levels of the theory, respectively, as compared with the recent experimental measurement by Hunter and Lias¹² of 207 ± 1 kcal/mol. Recall that Mayor-López et al.⁵⁰ have found a proton affinity of 217.7 kcal/mol for this structure at the CCSD(T) level of theory with a double- ζ basis set including polarization.

C. Ferrocene $\cdots Li^+$. Figure 2 shows the four stationary points that we have been able to characterize on the B3LYP potential energy surface of $Cp_2Fe \cdots Li^+$. Notice that akin to the protonated case, both the ring-bonded and the metal-bonded structures are stable for the case of the lithium cation. Our best calculation suggests that the ring-bonded form is more stable than the metal-bonded form for the ferrocene $\cdots Li^+$ complex.

We have also calculated the standard Gibbs energy of the dissociation reaction



for the two stable isomers of the ferrocene–lithium cation. For $T = 298$ K this quantity is known as the lithium cation basicity (LCB) of ferrocene. Our best LCB values are 37.4 and 29.4 kcal/mol for the isomers **1** and **2** of Figure 2, respectively. Hence our calculations predict that **1** is 6 kcal/mol more stable than **2**. According to the recent compilation of LCB values of Burke et al.,¹³ ferrocene is predicted to be a moderately strong basis toward the lithium cation.

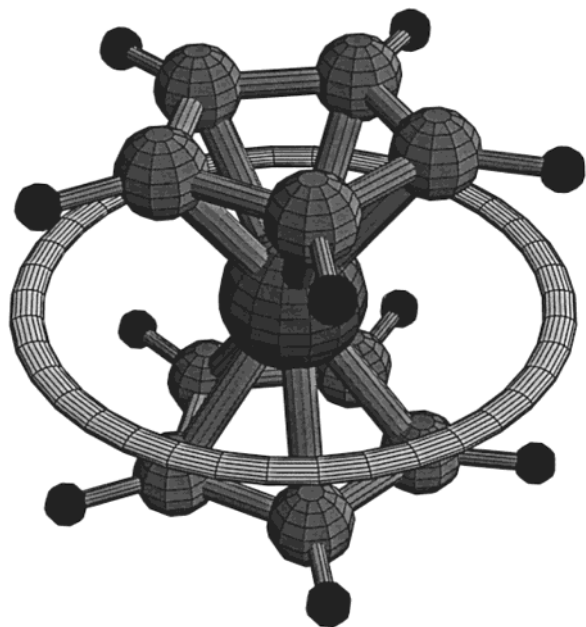


Figure 3. The orbit of the lithium cation in terms of a tube following the minimum energy path. The radius of the tube covers energy 30% higher than the energy barrier associated with the transition state **TS22**.

Table 3. Distances, in Å, from Iron to the Most Distant Carbon, *d*, and to the Closest Carbon, *c*, in Protonated Ferrocene ($\text{Cp}_2\text{Fe}\cdots\text{H}^+$) and in the Ferrocene–Lithium Cation Complex ($\text{Cp}_2\text{Fe}\cdots\text{Li}^+$)

structure	B3LYP/DZVP		B3LYP/TZVP+G(3df,2p)		
	<i>c</i>	<i>d</i>	<i>c</i>	<i>d</i>	
$\text{Cp}_2\text{Fe}\cdots\text{H}^+$	1	2.049	2.123	2.054	2.137
	TS11	1.998	2.095	2.007	2.104
	2	2.071	2.090	2.081	2.101
$\text{Cp}_2\text{Fe}\cdots\text{Li}^+$	1	2.049	2.049	2.069	2.069
	2	2.073	2.095	2.087	2.098
	TS12	2.046	2.091	2.054	2.107
	TS22	2.074	2.096	2.090	2.103

Nevertheless, it is worth noting that these two stable structures are separated by a transition state (structure **TS12** in Figure 2) with a barrier of 25.06 kcal/mol. This barrier seems to be high enough to provide both **1** and **2** with substantial kinetic stability toward interconversion. Indeed, since the barrier is only 5 kcal/mol less than the dissociation energy of **2**, interconversion between **1** and **2** will likely result in the fragmentation of the complex.

The metal-bonded isomer of $\text{Cp}_2\text{Fe}\cdots\text{Li}^+$ lies 8.52 kcal/mol higher in energy than the ring-bonded isomer. The lithium cation is at a distance of 2.4 Å from the central iron atom in a staggered arrangement with respect to both cyclopentadienyl rings. Remarkably, this structure constitutes a pure *planetary system* with the lithium cation *orbiting* around the ferrocene on a *planar* orbit. Observe from Figure 2 that the transition state connecting any two adjacent equivalent forms of **2** is separated by a barrier of only 2.6 kcal/mol through structure **TS22**, in which the lithium cation is at 2.53 Å from the central iron atom and eclipsed with respect to both cyclopentadienyl rings. To our knowledge this is the first *planetary system* found up to date having one and only one *planar* orbit. Figure 3 shows the orbit in terms of tube following the minimum energy path with a tube radius covering an energy 30% higher than the energy barrier associated with **TS22**.

Table 3 collects the distances from the central iron atom of the ferrocene moiety to the most distant carbon atom and to the closest carbon atom of the cyclopentadienyl ring nearest to

the metal, in both the protonated ferrocene and the ferrocene–lithium cation complex. Its inspection reveals that both basis sets yield very similar optimum distances. This adds to the mounting evidence that optimization at the B3LYP/DZVP level is quite reliable,³⁵ even for large molecules.

One more interesting feature that stems from Table 3 is that the ferrocene moiety distorts more appreciably upon complexation with H^+ than with Li^+ . Recall that our best optimum iron carbon distance in bare eclipsed ferrocene is 2.078 Å. Protonated ferrocene largest (2.137 Å) and shortest (2.054 Å) optimum iron carbon distances of the stable structure **1** of Figure 1 bracket loosely the unperturbed iron carbon distance of ferrocene. However, the largest (2.098 Å) and shortest (2.089 Å) optimum iron carbon distances of the stable ferrocene–lithium cation complex, structure **2** of Figure 2, represent a tight upper bound to the unperturbed iron carbon distance. This is supportive of the weaker interaction of Li^+ with ferrocene relative to H^+ .

The minimum energy of the most stable ferrocene–lithium cation complex isomer, structure **1** of Figure 2, has an iron carbon distance of 2.069 Å, only 0.01 Å shorter than the unperturbed ferrocene iron carbon optimum distance. Again, this indicates that Li^+ distorts very little the ferrocene moiety.

V. Conclusions

The interaction of ferrocene with both H^+ and Li^+ has been studied by using the B3LYP approximate hybrid density functional and an extended basis set. Our calculations predict that the most stable isomer of protonated ferrocene can be best viewed as a two electron-three center hydrogen bonded species, where the hydrogen binds the central iron atom with a carbon atom of one of the cyclopentadienyls. However, this species has been found to be fluxional for the metal protonated isomer lies 1.4 kcal/mol higher in energy. Additionally we have also been able to characterize the transition state for the hopping of the hydrogen from one carbon atom to an adjacent one on the same cyclopentadienyl. This structure lies 18.8 kcal/mol higher in energy than the stable protonated ferrocene.

We have predicted that the ferrocene–lithium cation complex has at least two stable isomers, separated by a transition state with an energy barrier of 25.06 kcal/mol. In both isomers Li^+ does not distort notably the ferrocene structure.

The most stable structure has the lithium cation bonded *on-top* one of the cyclopentadienyls, while in the other isomer lithium binds to the central iron atom. This isomer is in fact a *planetary system* in the sense that Li^+ has one and only one accessible *orbit* around the central ferrocene moiety, for adjacent equivalent structures of Li^+ around the ferrocene are separated by a barrier of only 2.6 kcal/mol.

The lithium cation gas-phase basicity is 37.4 kcal/mol for the most stable isomer and 29.4 kcal/mol for the next stable isomer of the ferrocene–lithium cation complex, respectively, at the B3LYP/TZVP+G(3df,2p) level of theory. These predictions await experimental verification.

Acknowledgment. This research was funded by Euskal Herriko Unibertsitatea (the University of the Basque Country), Gipuzkoako Foru Aldundia (the Provincial Government of Guipuzkoa), and Eusko Jaurlaritza (the Basque Government).

Supporting Information Available: A table of vibrational frequencies (PDF). This material is available free of charge via the Internet at <http://pubs.acs.org>.